



Wavefront-corrected post-compression of a 100-TW Ti:sapphire laser

Ji In Kim,^{1,2} Jin Woo Yoon,^{1,3}  Jeong Moon Yang,¹ Yeong Gyu Kim,¹  Jae Hee Sung,^{1,3} Seong Ku Lee,^{1,3,4}  and Chang Hee Nam^{1,2,5} 

¹Center for Relativistic Laser Science, Institute for Basic Science, Gwangju 61005, Republic of Korea

²Department of Physics and Photon Science, GIST, Gwangju 61005, Republic of Korea

³Ultraintense Laser Laboratory, Advanced Photonics Research Institute, GIST, Gwangju 61005, Republic of Korea

⁴lsk@gist.ac.kr

⁵chnam@gist.ac.kr

Abstract: We analyzed and corrected the wavefront distortion induced during the post-compression of a 100-TW Ti:Sapphire laser and achieved the intensity enhancement. In the post-compression, the spectral broadening of the laser was obtained by propagating through three 0.5 mm-thick fused silica plates and the laser pulse duration was post-compressed from 24 fs to 11 fs using a set of chirped mirrors. We measured the wavefront aberrations due to the intensity-dependent nonlinear process during the post-compression of femtosecond high-power laser pulses. By compensating for the wavefront aberrations with an adaptive optics system, the Strehl ratio of the post-compressed beam was improved from 0.37 to 0.52 and the focused intensity of the post-compressed beam could be enhanced by a factor of 1.5, while the enhancement without the wavefront correction was only a factor of 1.1 in spite of the peak-power enhancement by a factor of 1.8.

© 2022 Optica Publishing Group under the terms of the [Optica Open Access Publishing Agreement](#)

1. Introduction

As ultrahigh intensity lasers have been developed with the chirped pulse amplification (CPA) technique [1] and the adoption of a broadband gain medium, such as Ti:Sapphire, the output power of ultrashort CPA lasers reached the petawatt (PW) level in a number of institutes around the world [2], and recently the laser intensity of 10^{23} W/cm² has been demonstrated by tightly focusing a wavefront-corrected multi-PW laser [3,4]. Ultrahigh intensity lasers have been utilized for the investigation of strong field physics, such as laser-driven charged particle acceleration and strong field quantum electrodynamics [5–7].

The post-compression of ultrashort high-power lasers is a promising technique to enhance the power of CPA lasers through the spectral broadening by third-order nonlinear processes, such as self-phase modulation (SPM) [8,9]. Mourou *et al.* proposed to improve laser power through pulse shortening by utilizing a large aperture solid plate as a nonlinear medium with a quasi-flat top Joule level beam [10]. Ginzburg *et al.* reported that the pulse duration of the laser beam with an 18-J energy is shortened from 64 fs to 11 fs with 1.5 PW peak-power through the post-compression [11]. Shaykin *et al.* demonstrated that the pulse duration of the laser beam reached 10 fs using a 4-mm-thick KDP crystal [12]. The post-compression using solid plate showed effective temporal compression performance in Joule-level femtosecond lasers [13].

Since laser intensity at focus is one of the most critical parameters in deciding the physical interaction regime, the wavefront quality of a post-compressed beam must be properly managed. In the post-compression process including free propagation, the spatial quality can be degraded by the wavefront distortion induced during the spectral broadening in the case of a non-uniform beam due to the intensity-dependent third-order nonlinearity. This wavefront distortion can result

in self-focusing and may lead to the damage of optical components. More importantly, it can lead to the degradation of focused laser intensity due to the wavefront distortion. To avoid the optical damage by self-focusing, spatial filtering [14] or self-filtering [13] has been adopted. However, these filtering methods are not effective in suppressing wavefront aberrations, since they cannot remove the slowly varying phase modulation induced by low frequency intensity modulation in the beam. In order to correct the wavefront distortion and thus to improve the focused intensity, an adaptive optics system with a deformable mirror (DM) can be employed. Druon *et al.* demonstrated that the DM effectively compensated for a Gaussian-shaped aberration induced by focusing a 5 mJ laser with a Gaussian intensity profile into a glass, improving the Strehl ratio [15]. Besides, Ginzburg *et al.* theoretically showed that the Strehl ratio of a laser beam with 50% modulation in the center can be improved through the correction of low-order aberrations, which can be corrected by a DM [16].

In this paper, we carried out the wavefront-corrected post-compression of a 100-TW Ti:Sapphire laser and demonstrated the enhancement of laser intensity at focus. In our previous work [14], we showed the post-compression of a 100-TW laser to enhance the peak-power. We examined here the wavefront distortion induced during the spectral broadening in a nonlinear medium that affects the focusability of post-compressed laser pulses. After the post-compression using fused silica plates and a set of chirped mirrors, the pulse duration of the laser pulses was shortened from 24 fs to 11 fs. The wavefront aberration induced in the nonlinear plate was measured with a wavefront sensor (WFS), and an adaptive optical system with DM and WFS was employed to correct the aberrations. Through the wavefront correction, the focal spot was recovered with the Strehl ratio of 84% of that of the input beam, showing that the post-compression with wavefront correction enhanced the peak intensity of a post-compressed laser.

2. Post-compression of a 100-TW laser

The post-compression of a 24 fs, 100-TW Ti:Sapphire laser has been performed using the setup in Fig. 1 [17]. In the post-compression process, the laser beam from the pulse compressor was spectrally broadened by propagating through three 0.5 mm-thick fused silica plates and recompressed with a set of chirped mirrors (UltraFast Innovations) to compensate for the dispersion induced by the plates. The reflectivity of the chirped mirror is over 99% in the spectral range from 600 to 950 nm and the group delay dispersion (GDD) is -100 fs^2 per a pair of the mirrors. The beam diameter, fluence and intensity of the laser beam on the chirped mirrors were 70 mm, 14 GW/cm^2 , and 0.34 mJ/cm^2 , respectively, after the energy attenuation by two uncoated glass wedges. For the characterization of post-compressed pulses, the laser beam was de-magnified to 6 times with two silver-coated concave mirrors and attenuated to 4×10^{-5} using uncoated glasses to avoid nonlinear effects in the 1-mm thickness vacuum window by keeping the B-integral of the window to be much smaller than 1. The temporal characteristics of post-compressed pulses were measured with spectral phase interferometry for direct electric-field reconstruction (SPIDER). The dispersion induced by the vacuum window and the air in the optical beam path to the SPIDER, corresponding to GDD of 104 fs^2 , was almost compensated by the chirped mirrors.

The input and the output spectra are shown in Fig. 2(a) with the black and the red lines, respectively, which shows that the spectral width was almost doubled after the three fused silica plates. The laser intensity and the beam diameter on the plates were 2.6 TW/cm^2 and 70 mm, respectively. The B-integral for the three plates was 6.5. Figure 2(b) shows the measured temporal profiles of the input and the post-compressed pulses. We achieved the pulse shortening from 24 fs to 11 fs (FWHM) and the peak-power was enhanced by 1.8 times, as shown in Fig. 2(b). In this plot, the energy loss at the uncoated fused silica plates was not considered since it can become minimal by implementing anti-reflection coated plates or by setting them at the Brewster's angle. Although the peak-power of the laser beam was improved due to the pulse shortening

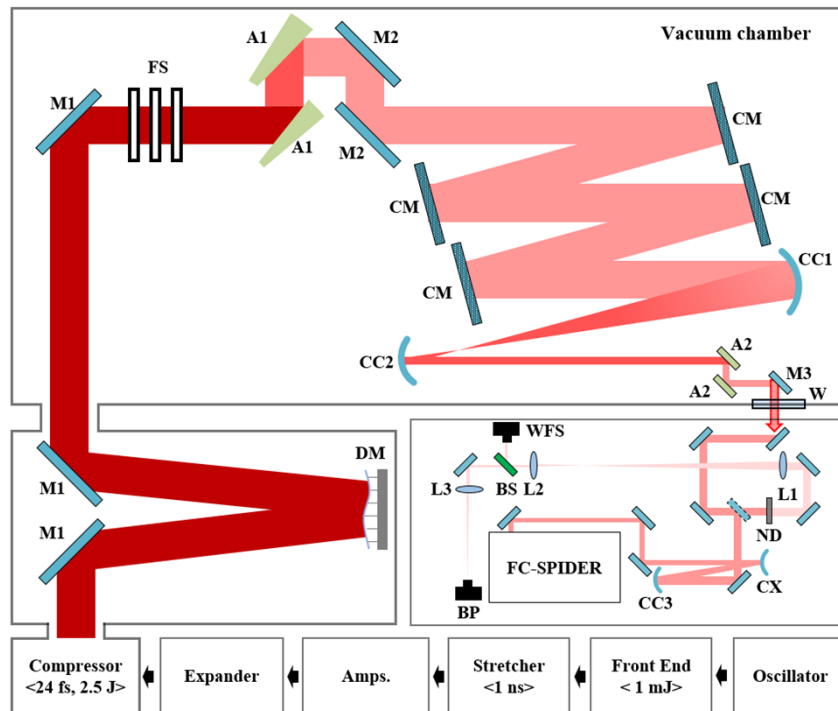


Fig. 1. Schematics of the experimental setup for the post-compression with wavefront correction. M1: dielectric mirror, FS: fused silica plates for spectral broadening, A1 and A2: uncoated glass for attenuation of pulse's energy, M2, M3, and mirrors at diagnostics: silver-coated mirror, CM: chirped mirror, CC (CC1, CC2, and CC3) and CX: silver-coated concave and convex mirrors, W: chamber window, L: AR-coated achromatic lens, ND: a neutral density filter, BS: beam splitter, WFS: wavefront sensor and BP: CMOS beam profiler.

by post-compression, the intensity enhancement at focus should be carefully assessed since the wavefront of a post-compressed beam may become distorted during the SPM process.

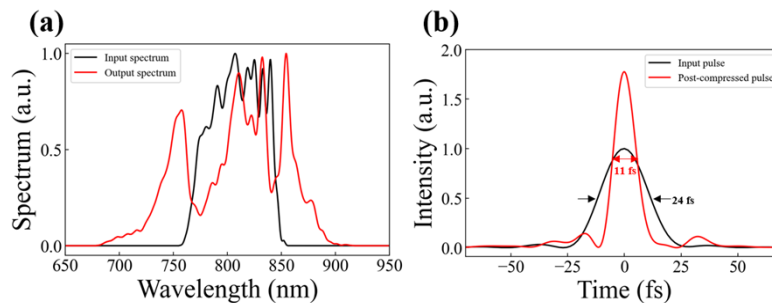


Fig. 2. (a) Broadened spectrum (red line) after three 0.5-mm fused silica plates, shown along with the input spectrum (black line). (b) Temporal profiles of the post-compressed pulse (red line) and the input pulse (black line) measured with a SPIDER. The area of the two pulses is set to be the same.

3. Wavefront correction and intensity enhancement of post-compressed pulses

3.1. Measurement and correction of the wavefront of post-compressed pulses

During the spectral broadening in a thin solid medium, the wavefront of a laser pulse can be degraded due to intensity-dependent third-order nonlinearity. We measured the wavefront of post-compressed laser pulses using the WFS and corrected the degraded wavefront by employing an adaptive optics system. The DM was installed before the plates to pre-compensate for the wavefront distortion incurred during the post-compression. The location of the DM was chosen to avoid an accidental damage of the DM due to self-focusing when placed after the post-compression stage.

For the analysis of beam quality, the wavefront and the focal spot image of post-compressed laser pulses were measured. The laser beam after the fused silica plates was image-relayed to a WFS (SID4, Phasics) with a set of achromatic lenses ($f = 750$ mm and $f = 200$ mm). The focal spot image was measured using a CMOS camera after focusing with an achromatic lens ($f = 300$ mm). The wavefront aberrations measured with the WFS were then corrected with an adaptive optics system, consisting of a 70-mm DM (AKA optics) with 32 actuators and the WFS for a feedback control. An optimization process to minimize the wavefront aberrations was performed at 0.1 Hz.

In order to change the input energy without affecting spatial characteristics, the combination of a high-quality half-wave plate and a polarizer, installed after the amplification stage of the 100-TW system, was used to adjust the laser energy by rotating the wave plate. In order to confirm that the spatial characteristics of the input beam did not change when the input beam energy was controlled, we measured the beam profiles and the wavefronts without the plates for the cases of the low energy (0.03 J) and the high energy (2.5 J). The beam profiles, as shown in Figs. 3(a) and (b), for the low and the high energy beams without the plates exhibit no significant difference. The wavefronts for the low and the high energy beams without the plates are shown in Figs. 3(c) and (d), obtained after averaging over three shots, respectively. The wavefront difference between the two beams, obtained by subtracting the wavefront of the low energy beam from that of the high energy beam, was 0.02 μm (rms). The measurement of the beam profiles and wavefronts, thus, confirmed that no significant difference in the spatial characteristics was induced during the control of input beam energy.

The wavefront aberrations were corrected in two steps. Firstly, the wavefront aberrations at the low laser energy of 0.03 J (B-integral < 0.1) were corrected with the adaptive optics system to remove the initial aberrations of the laser beam after passing through the fused silica plates. By correcting the wavefront at the low energy, the wavefront error was optimized to 0.037 μm (rms), as shown in Fig. 3(f). Secondly, at the laser energy of 2.5 J, the induced wavefront aberrations of post-compressed laser pulses were measured with the WFS. The measurement result showed that the wavefront aberrations were considerably induced during the nonlinear process in the plates. The wavefront error increased to 0.086 μm (rms), implying a degraded focal spot quality. In order to improve the distorted wavefront, the wavefront correction was carried out using the adaptive optics system. Figure 3(h) shows the corrected wavefront at the high energy. The wavefront error was improved to 0.056 μm (rms), but still larger than that of the low energy case. In addition, it is noted that the wavefront in Fig. 3(g) after the nonlinear plates closely followed the input beam profile, shown in Fig. 3(e), of the 100-TW laser, which clearly supports that the wavefront distortion came from the nonlinear spectral broadening process.

We analyzed the wavefront of the high energy case to figure out the source of the remnant wavefront aberrations. Considering only the first 13 orders of Zernike polynomials, we compared the wavefront maps for the low-order aberrations before and after the wavefront correction, as shown in Figs. 3(i) and (j). In this case, the wavefront error decreased from 0.075 μm to 0.036 μm after the correction. On the other hand, the wavefront error containing the high-order aberrations,

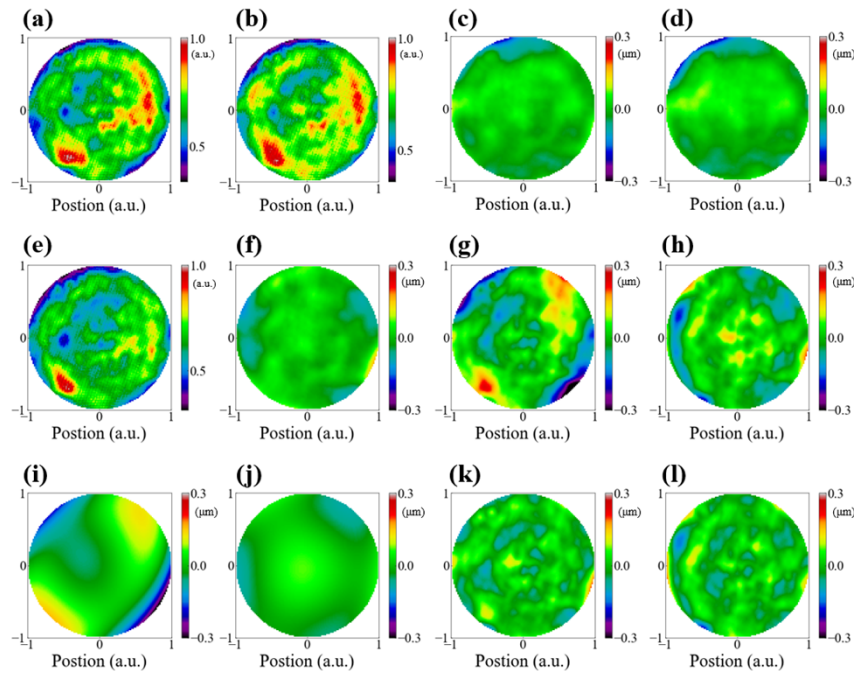


Fig. 3. Beam profile and wavefront: (a)-(d), measured without the fused silica plates, and (e)-(l), measured after propagating through the plates. Beam profiles for (a) the low energy (0.03 J) and (b) the high energy (2.5 J). Wavefronts for (c) the low energy and (d) the high energy. (e) Beam profile and (f) wavefront of the low energy case, showing the undistorted wavefront. (g) Uncorrected wavefront and (h) corrected wavefront of a post-compressed pulse with the high energy case. (i) and (j) Wavefront maps with low-order aberration components of (g) and (h), respectively. (k) and (l) Wavefront maps with high-order aberration components of (g) and (h), respectively.

i.e., the remnant part of the wavefront map after subtracting the low-order aberrations (the first 13 orders), showed no significant difference after the correction, as shown in Figs. 3(k) and (l). This means that the high-order wavefront aberrations could not be corrected with the DM, showing the limitation of our DM with 32 actuators. This high-order wavefront distortion can be mitigated by installing a spatial filtering system [14] or replacing the DM with a higher-spatial-resolution DM.

3.2. Intensity enhancement of post-compressed pulses

The degradation of the laser wavefront after the post-compression affects the laser intensity achievable at focus. Though the peak-power could be enhanced through the post-compression, as shown in Fig. 2(b), the focused intensity cannot be improved as much, since the focal spot quality can deteriorate due to the wavefront aberrations shown in Figs. 3(g) and 3(h). Thus, focal spot images were measured and analyzed to investigate the intensity enhancement at the focus for the three cases: a low energy beam with an undistorted wavefront, a high energy beam without correction, and a high energy beam with correction. The initial focal spot image in the low energy case after removing the initial wavefront error is shown in Fig. 4(a), and the peak intensity at the focal spot was 0.62 of its diffraction-limited case for the input beam profile with a flat phase. In the calculation of the focal spot image of the diffraction-limited beam, the Fresnel propagation using a two-step method in the AO tool package [18] was implemented for the focusing of a laser beam with a lens with $f = 300$ mm at 800 nm. The focal spot image became degraded in the case of the energy of 2.5 J, as shown in Fig. 4(b), since the considerable wavefront distortion

was induced during the post-compression process. This resulted in a significant decrease of the Strehl ratio to 0.37. On the other hand, after additional compensation of the induced wavefront error during the post-compression, the focal spot image was recovered, as shown in Fig. 4(c), and the Strehl ratio was improved to 0.52. The lineout profiles of the diffraction-limited focal spot (black dotted line) and the measured focal spot (red line) for each case are shown in Figs. 4(d), (e), and (f), where the peak value of the diffraction-limited focal spot was normalized to 1. Our result thus showed that, even in the case of a non-uniform laser beam, the wavefront-corrected post-compression could effectively improve the intensity at the focus.

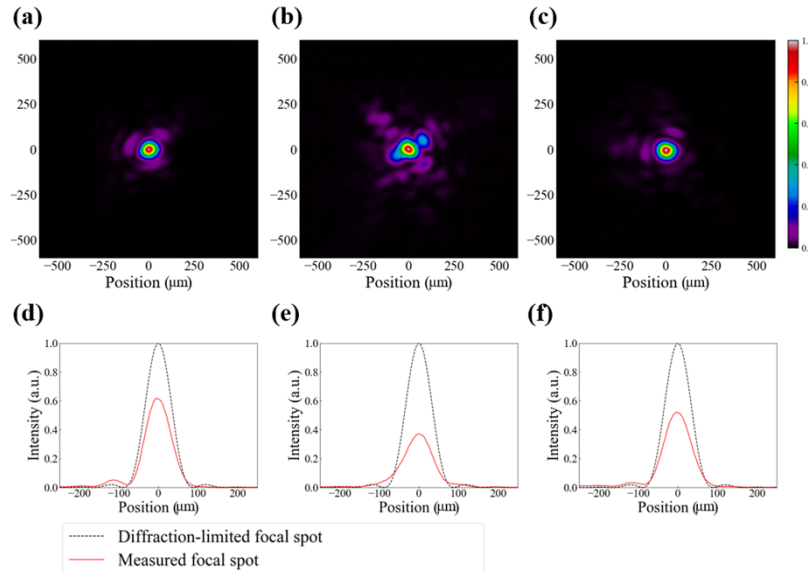


Fig. 4. Comparison of focal spot images: (a) at a low input energy (0.03 J), (b) at a high input energy (2.5 J), and (c) at the high input energy after the wavefront correction. (d), (e), and (f) Lineout profiles along the horizontal axis for the diffraction-limited and the measured focal spots of (a), (b), and (c), respectively.

Although the intensity at the focus could increase by a factor of 1.8 by pulse shortening through the post-compression, the peak intensity increased only 1.1 times without wavefront correction because the Strehl ratio decreased from 0.62 to 0.37 due to the wavefront aberration. Whereas, by the wavefront correction with the adaptive optics system, the peak intensity could be enhanced by 1.5 times after improving the Strehl ratio from 0.37 to 0.52, corresponding to 84% of that of the undistorted input beam. We note that the application of the reduced energy to the chirped mirrors was imposed to avoid the strong nonlinear absorption [19] by the chirped mirrors. We observed that the reflectance of the chirped mirrors decreased when the intensity of 25 fs laser pulses exceeded 0.5 TW/cm^2 . When a full energy laser pulse was applied to the chirped mirrors, more than a half of the laser energy was lost due to the nonlinear absorption by the chirped mirrors. In order to compress the full energy beam, the beam size should be enlarged more than two times, or a new design of chirped mirrors supporting higher laser intensity has to be developed. Besides, the spatio-temporal coupling of post-compressed pulses may affect the focused laser intensity. In our experimental results, the measured pulse duration (11.0 fs, FWHM) was close to the Fourier transform-limited pulse duration (10.3 fs) and the measured focal spot size (75 μm , FWHM) was almost the same as the diffraction-limited focal spot size (74 μm), which indicates that the spatio-temporal coupling was not so significant in our post-compressed laser pulses. As a future work, we are planning to perform a systematic measurement of spatio-temporal coupling.

4. Conclusion

The peak-intensity enhancement through post-compression has been investigated with the wavefront correction using an adaptive optics system in a 100-TW Ti:Sapphire laser. The laser pulse was shortened from 24 fs to 11 fs by the post-compression achieved by employing thin fused silica plates and a set of chirped mirrors. The wavefront aberrations, coming from the propagation of a non-uniform beam through the nonlinear plates, were measured and corrected using a DM. The Strehl ratio was improved from 0.37 to 0.52 after the wavefront correction. Through the wavefront-corrected post-compression, the focused intensity of the 100-TW Ti:Sapphire laser could be enhanced by 1.5 times, while the enhancement of the uncorrected case was a factor of 1.1, showing that the wavefront distortion induced in the plates degraded the focusability of post-compressed laser pulses. Our results confirmed the necessity of the wavefront-correction process in the post-compression of a femtosecond high-power laser. More importantly, our results showed clearly that the implementation of the post-compression technique to PW or multi-PW lasers should be proceeded with well-managed wavefront control due to their considerably more complicated optical structure with large-size optical components in order to realize unprecedented laser power and intensity for the exploration of strong field physics under extreme physical conditions.

Funding. Institute for Basic Science (IBS-R012-D1); Gwangju Institute of Science and Technology (Ultrashort Quantum Beam Facility operation program (140011) through Advanced Photonics Research Institute).

Disclosures. The authors declare no conflicts of interest.

Data availability. Data underlying the results presented in this paper are not publicly available at this time but may be obtained from the authors upon reasonable request.

References

1. D. Strickland and G. Mourou, "Compression of amplified chirped optical pulses," *Opt. Commun.* **56**(3), 219–221 (1985).
2. C. N. Danson, C. Haefner, J. Bromage, T. Butcher, J.-C. F. Chanteloup, E. A. Chowdhury, A. Galvanauskas, L. A. Gizzi, J. Hein, D. I. Hillier, N. W. Hopps, Y. Kato, E. A. Khazanov, R. Kodama, G. Korn, R. Li, Y. Li, J. Limpert, J. Ma, C. H. Nam, D. Neely, D. Papadopoulos, R. R. Penman, L. Qian, J. J. Rocca, A. A. Shaykin, C. W. Siders, C. Spindloe, S. Szatmári, R. M. G. M. Trines, J. Zhu, P. Zhu, and J. D. Zuegel, "Petawatt and exawatt class lasers worldwide," *High Power Laser Sci. Eng.* **7**, e54 (2019).
3. J. W. Yoon, Y. G. Kim, I. W. Choi, J. H. Sung, H. W. Lee, S. K. Lee, and C. H. Nam, "Realization of laser intensity over 10^{23} W/cm²," *Optica* **8**(5), 630–635 (2021).
4. J. H. Sung, H. W. Lee, J. Y. Yoo, J. W. Yoon, C. W. Lee, J. M. Yang, Y. J. Son, Y. H. Jang, S. K. Lee, and C. H. Nam, "4.2 PW, 20 fs Ti:sapphire laser at 0.1 Hz," *Opt. Lett.* **42**(11), 2058 (2017).
5. I. J. Kim, K. H. Pae, C. M. Kim, H. T. Kim, J. H. Sung, S. K. Lee, T. J. Yu, I. W. Choi, C.-L. Lee, K. H. Nam, P. V. Nickles, T. M. Jeong, and J. Lee, "Transition of Proton Energy Scaling Using an Ultrathin Target Irradiated by Linearly Polarized Femtosecond Laser Pulses," *Phys. Rev. Lett.* **111**(16), 165003 (2013).
6. H. T. Kim, K. H. Pae, H. J. Cha, I. J. Kim, T. J. Yu, J. H. Sung, S. K. Lee, T. M. Jeong, and J. Lee, "Enhancement of Electron Energy to the Multi-GeV Regime by a Dual-Stage Laser-Wakefield Accelerator Pumped by Petawatt Laser Pulses," *Phys. Rev. Lett.* **111**(16), 165002 (2013).
7. A. Di Piazza, C. Müller, K. Z. Hatsagortsyan, and C. H. Keitel, "Extremely high-intensity laser interactions with fundamental quantum systems," *Rev. Mod. Phys.* **84**(3), 1177–1228 (2012).
8. A. Fisher, P. L. Kelley, and T. K. Gustafson, "Subpicosecond pulse generation using the optical Kerr effect," *Appl. Phys. Lett.* **14**(4), 140–143 (1969).
9. A. Laubereau, "External Frequency Modulation and Compression of Picosecond Pulses," *Phys. Lett.* **29**(9), 539–540 (1969).
10. G. Mourou, S. Mironov, E. Khazanov, and A. Sergeev, "Single cycle thin film compressor opening the door to Zeptosecond-Exawatt physics," *Eur. Phys. J. Spec. Top.* **223**(6), 1181–1188 (2014).
11. V. Ginzburg, I. Yakovlev, A. Kochetkov, A. Kuzmin, S. Mironov, I. Shaikin, A. Shaykin, and E. Khazanov, "11 fs, 1.5 PW laser with nonlinear pulse compression," *Opt. Express* **29**(18), 28297–28306 (2021).
12. A. Shaykin, V. Ginzburg, I. Yakovlev, A. Kochetkov, A. Kuzmin, S. Mironov, I. Shaikin, S. Stukachev, V. Lozhkarev, A. Prokhorov, and E. Khazanov, "Use of KDP crystal as a Kerr nonlinear medium for compressing PW laser pulses down to 10 fs," *High Power Laser Sci. Eng.* **9**, e54 (2021).
13. E. A. Khazanov, S. Y. Mironov, and G. Mourou, "Nonlinear compression of high-power laser pulses: compression after compressor approach," *Phys.-Usp.* **62**(11), 1096–1124 (2019).

14. J. I. Kim, Y. G. Kim, J. M. Yang, J. W. Yoon, J. H. Sung, S. K. Lee, and C. H. Nam, "Sub-10 fs pulse generation by post-compression for peak-power enhancement of a 100-TW Ti:Sapphire laser," *Opt. Express* **30**(6), 8734–8741 (2022).
15. F. Druon, G. Chériaux, J. Faure, J. Nees, M. Nantel, A. Maksimchuk, G. Mourou, J. C. Chanteloup, and G. Vdovin, "Wave-front correction of femtosecond terawatt lasers by deformable mirrors," *Opt. Lett.* **23**(13), 1043–1045 (1998).
16. V. Ginzburg, I. Yakovlev, A. Zuev, A. Korobeynikova, A. Kochetkov, A. Kuzmin, S. Mironov, A. Shaykin, I. Shaikin, E. Khazanov, and G. Mourou, "Fivefold compression of 250-TW laser pulses," *Phys. Rev. A* **101**(1), 013829 (2020).
17. J. H. Sung, J. W. Yoon, I. W. Choi, S. K. Lee, H. W. Lee, J. M. Yang, Y. G. Kim, and C. H. Nam, "5-Hz, 150-TW Ti:sapphire Laser with High Spatiotemporal Quality," *J. Korean Phys. Soc.* **77**(3), 223–228 (2020).
18. M. J. Townson, O. J. D. Farley, G. Orban de Xivry, J. Osborn, and A. P. Reeves, "AOTools: a Python package for adaptive optics modelling and analysis," *Opt. Express* **27**(22), 31316 (2019).
19. G. Gui, A. Adak, M. Dandapat, D. Carlson, D. Morrill, A. Guggenmos, H. Kapteyn, M. Murnane, V. Pervak, and C.-T. Liao, "Measurement and control of optical nonlinearities in dispersive dielectric multilayers," *Opt. Express* **29**(4), 4947–4957 (2021).